

POWER OUTPUT AND PROPULSIVE EFFICIENCY OF SWIMMING BOTTLENOSE DOLPHINS (*TURSIOPS TRUNCATUS*)

FRANK E. FISH

Department of Biology, West Chester University, West Chester, PA 19383, USA

Accepted 12 August 1993

Summary

The power output and propulsive efficiency of swimming bottlenose dolphins (*Tursiops truncatus*) were determined from a hydromechanical model. The propulsive movements were filmed as dolphins swam in large pools. Dolphins swam at velocities of 1.2–6.0 ms⁻¹. Propulsion was provided by dorsoventral oscillations of the posterior body and flukes. The maximum angle of attack of the flukes showed a linear decrease with velocity, whereas the frequency of the propulsive cycle increased linearly with increasing velocity. Amplitude was 20% of body length and remained constant with velocity. Propulsive efficiency was 0.81. The thrust power computed was within physiological limits. After correction for effects due to swimming depth, the coefficient of drag was found to be 3.2 times higher than the theoretical minimum assuming turbulent boundary conditions. The motions of the body and flukes are primarily responsible for the increased drag. This analysis supports other studies that indicate that bottlenose dolphins, although well adapted for efficient high-performance swimming, show no unusual hydrodynamic performance.

Introduction

Most studies of dolphin swimming energetics and hydrodynamics have used models based on rigid bodies. These models assumed that the thrust generated by swimming dolphins was equal to estimates of drag from gliding dolphins (Lang and Daybell, 1963; Lang and Pryor, 1966), towed reproductions of dolphins (Purves *et al.* 1975; Aleyev, 1977) and simple hydrodynamic formulae based on flat plates (Gray, 1936; Hui, 1987). However, a dolphin does not swim as a rigid body, but oscillates its tail and flukes in large-amplitude motions for propulsion (Slijper, 1961; Lang and Daybell, 1963; Videler and Kamermans, 1985). Hydromechanical models based on kinematics provided values of power output for actively swimming animals which exceeded those for equivalent rigid bodies by 3–7 times (Lighthill, 1971; Webb, 1975; Fish *et al.* 1988). Estimates of drag based on rigid-body analogies, therefore, may underestimate the energy expenditure of swimming by dolphins. Such underestimates led researchers to look for special mechanisms that might minimize drag and enable the dolphins to perform better than

Key words: dolphin, swimming, hydrodynamics, power output, *Tursiops truncatus*.

engineered designs (Gray, 1936; Kramer, 1960). In reviewing the available literature on dolphin swimming performance, Fish and Hui (1991) found no evidence for drag reduction from special mechanisms. Although current understanding was incomplete, they concluded that dolphin body design and behavior decrease swimming effort.

Hydromechanical models based on swimming kinematics are considered to be the only method with sufficient predictive value to calculate power output (Webb, 1975). Dolphins are good models for this type of analysis, because their swimming mode, subcarangiform with a lunate tail, effectively separates the structures associated with thrust production from those associated with drag production (Lighthill, 1969). Estimates of thrust based on the motion of the flukes can be used to assess independently the drag due to body form and that due to swimming motions. A number of studies have used kinematic data (Norris and Prescott, 1961; Lang and Daybell, 1963) to help develop hydromechanical models based on oscillating plates or hydrofoils (Parry, 1949; Lighthill, 1970; Wu, 1971; Chopra and Kambe, 1977; Yates, 1983). However, application of these models has relied on data from a single swimming speed for a single dolphin. Estimates of swimming energetics and hydrodynamics have come mainly from examinations of maximal swimming effort (Lang, 1975; Goforth, 1990) and have ignored submaximal swimming by dolphins. In the wild, dolphins swim over a wide range of speeds (Norris and Prescott, 1961; Wursig and Wursig, 1979; Au and Perryman, 1982; Lockyer and Morris, 1987). Because studies of dolphin swimming performance have not considered the full range of speeds, an incomplete picture of dolphin swimming energetics and hydrodynamics has emerged.

The purpose of the present study is to describe the kinematics of dolphins and to compute the thrust power, propulsive efficiency and drag over a wide range of swimming speeds. A hydromechanical model of lunate-tail propulsion will be used for the computations.

Materials and methods

Experimental animals

The swimming motions of five trained bottlenose dolphins (*Tursiops truncatus*) were filmed at Sea World in Orlando, Florida, and the National Aquarium in Baltimore, Maryland. Experiments were performed in large elliptical pools (Sea World: maximum length 27.4m; National Aquarium: maximum length 33.5m). The curved portions of each pool were constructed of glass panels. A water depth of 1.4–2.1m was visible through the panels. Depth of the pools was 7.3m and water temperature was maintained at 20–22°C.

Prior to each swimming bout, the animals were marked with zinc oxide reference points on the lateral aspects of the caudal peduncle. Dolphins swam along the curved wall of the pool routinely or under the direction of human trainers. All dolphins had been trained to swim near the water surface. The speed of the animals varied in response to cues from trainers.

Morphological measurements were obtained for each dolphin and are summarized in Table 1. Body length (L , m) is the linear distance from rostral tip to fluke notch and fluke

Table 1. *Morphometrics of dolphins (Tursiops truncatus) tested*

Dimension	Dolphin				
	Toad	Goofy	Nani	Nalu	Akai
Sex	Female	Female	Female	Male	Male
Age (years)	20	22	20	20	18
Body mass (kg)	192.8	263.1	229.5	228.2	211.4
Body length (m)	2.51	2.70	2.60	2.70	2.54
Maximum diameter (m)	0.49	0.58	0.52	0.48	0.48
Fineness ratio	5.10	4.69	5.00	5.63	5.34
Surface area (m ²)	2.99	2.45	2.74	2.73	2.60
Fluke span (m)	0.58	0.65	0.73	0.68	0.65
Planar fluke area (m ²)	0.089	0.117	0.112	0.110	0.105
Fluke chord (m)	0.21	0.28	0.21	0.21	0.20
Aspect ratio	3.78	3.61	4.69	4.20	4.00

span (S , m) is the linear distance between fluke tips. Planar surface area of flukes (F_a , m²) and maximum body diameter (D , m) were measured from scaled photographs. Aspect ratio of the flukes (AR) was calculated as S^2/F_a , and the root fluke chord (C , m) was measured as the centerline distance from leading to trailing edges of the flukes. Fineness ratio (FR) was calculated as L/D . Surface area of the body (S_a , m²) was calculated from a prediction equation dependent on body mass (M , kg):

$$S_a = 0.08M^{0.65}, \quad (1)$$

based on data from odontocetes (Slijper, 1958; Lang and Daybell, 1963, Lang and Pryor, 1966; Kanwisher and Sundnes, 1966; Hampton *et al.* 1971; Ridgway, 1972; Yasui, 1980; Andersen, 1981; Hui, 1987; Bose *et al.* 1990; D. P. Costa, unpublished results; Fig. 1).

Film analysis

Dolphins were filmed with either ciné or video cameras. Ciné films were made at 64frames s⁻¹ with a Bolex H-16 ciné camera equipped with a Kern Vario-Switar 100 POE zoom lens (1:1.9, f 16–100mm) using 16mm film (Kodak 4-X reversal film 7277, ASA 400). Film records were analyzed by sequentially projecting individual frames of film with a stop-action projector (Lafayette Instrument Co., model 00100) onto a digitizer tablet (GTCO, Digi-Pad 21A71D4) interfaced to an IBM PC microcomputer. Dolphin swimming was videotaped with a Panasonic Camcorder at 60Hz. Sequential body and fluke positions were digitized from individual frames of videotape with an AT-compatible computer, Panasonic AG-7300 video recorder, Sony PVM 1341 monitor and a video analysis system (Peak Performance Technologies, Inc.).

Data were acquired only from those film records in which dolphins swam steadily with no apparent accelerations and the dolphin maintained a horizontal path. From these records, average swimming velocity (U , m s⁻¹) was measured as the total displacement per cycle divided by the cycle duration. Steady swimming was achieved with a less than 10% difference in U between the first and second halves of a propulsive cycle and with an average difference of 4.9%. Stroke cycle frequency (f , Hz), peak-to-peak amplitude of

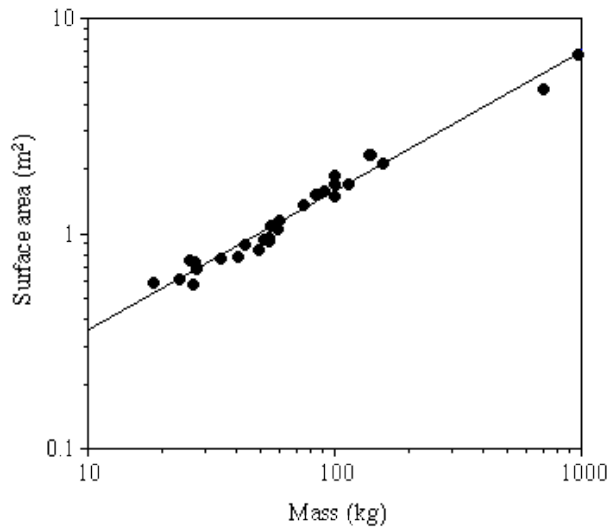


Fig. 1. Surface area (m^2) as a function of body mass (kg) for a variety of odontocetes (see text for references). Regression equation for line provided in text. Correlation coefficient for the line was 0.98 ($P < 0.01$).

the fluke motion (A , m) and angle of attack (α , rad) were measured. Angle of attack is the angle between the tangent of the flukes' path and the axis of the flukes (Fig. 2; Fierstine and Walters, 1968; Fish *et al.* 1988).

Reynolds numbers (Re) are based on the dolphin's length (L , m), swimming velocity (U) and the kinematic viscosity (ν) of sea water ($1.044 \times 10^{-6} \text{ m}^2 \text{ s}^{-1}$) using the equation:

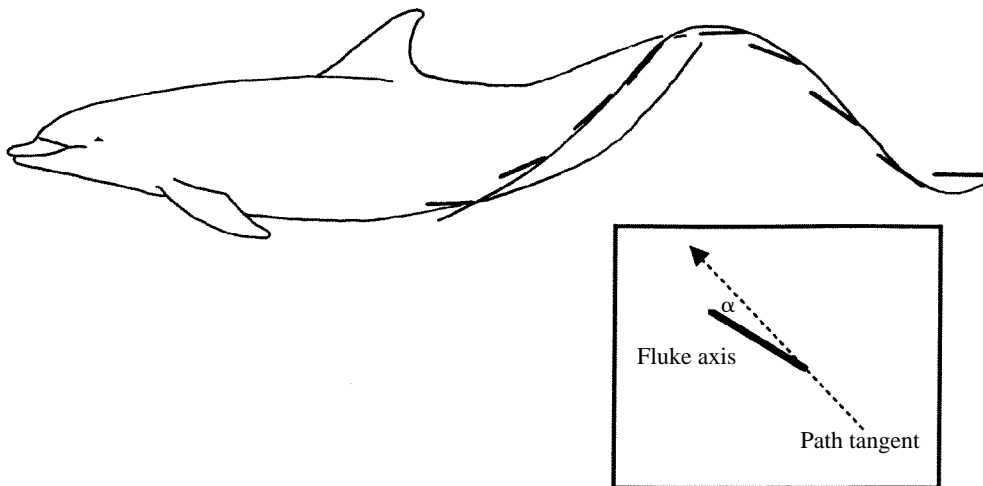


Fig. 2. Path and position of dolphin flukes throughout a stroke cycle. The tips of the flukes move along a sinusoidal path. Fluke position with respect to the path is shown as straight lines at intervals of 0.1s. The inset shows how the angle of attack was measured as the angle between the fluke axis and the tangent to the fluke pathway.

$$Re = LU/\nu . \quad (2)$$

Submersion depth (H) was measured from the surface to the centerline of the body.

Power output, efficiency and drag coefficient calculation

A hydromechanical model of lunate-tail propulsion based on unsteady wing theory (Chopra and Kambe, 1977; Yates, 1983) was used to calculate thrust power output (P_T), coefficient of drag (C_D), and propulsive efficiency (η). Propulsive efficiency is defined as the mean rate of work derived from mean thrust divided by the mean rate of all work that the animal is performing while swimming (Chopra and Kambe, 1977). In the model, the relationship between reduced frequency (σ) and proportional feathering parameter (θ) determines the coefficient of thrust (C_T) and η . The reduced frequency is a measure of the unsteady effects of flow about the flukes, and is:

$$\sigma = \omega C/U , \quad (3)$$

where ω is the radian frequency, equal to $2\pi f$ (Yates, 1983). The feathering parameter, θ , is the ratio of the maximum α to the maximum angle ($\omega h/U$) achieved by the pitching axis of the flukes (Yates, 1983) and is:

$$\theta = U\alpha_{\max}/\omega h . \quad (4)$$

The parameter h is the amplitude of heave (Yates, 1983) and was calculated from $A/2$.

The mean thrust power output (P_T) is given by:

$$P_T = 0.5\eta\rho C_T U^3 F_a (h/C)^2 , \quad (5)$$

where ρ is the density of sea water. For a body moving at constant U , P_T is equal to the power output expended in overcoming drag, and the dimensionless drag coefficient (C_D) is calculated as:

$$C_D = P_T/0.5\rho S_a U^3 . \quad (6)$$

Because dolphins swimming near the water surface would have experienced increased drag due to wave formation, a drag coefficient corrected for effects due to submergence depth (C_{Dd}) was calculated (Hertel, 1966, 1969; Au and Weihs, 1980; Blake, 1983) as:

$$C_{Dd} = C_D/\gamma . \quad (7)$$

The drag augmentation factor due to the influence of the water's surface, γ , varies with relative submergence depth of H/D . For a body of revolution, the range of γ is 1–5. A maximum value for γ occurs at $H/D=0.5$; minima occur at $-0.5 > H/D > 3$.

Results

Swimming speeds and kinematics

Morphological and hydrodynamically relevant dimensions of the five dolphins are provided in Table 1.

Fifty-six swimming sequences were filmed that were determined to be acceptable for

kinematic analysis. The dolphins swam steadily along the glass wall of the pool maintaining a distance of approximately 1–2m from the wall. Swimming depth was shallow at 0.40–3.52*D*. Dolphins swam at velocities ranging from 1.22 to 6.0 ms⁻¹ ($Re=3.16\times 10^6-15.3\times 10^6$). These velocities were within the range of burst and routine swimming speeds reported previously for dolphins (Lockyer and Morris, 1987; Fish and Hui, 1991). Maximum speed for *Tursiops* was lower than the maximum speed of 15 ms⁻¹ reported for wild *Tursiops* (Lockyer and Morris, 1987) and 8.3 ms⁻¹ for a 7.5 s burst measured by Lang and Norris (1966) for *Tursiops*. This difference in maximum speed is accounted for by the inverse relationship between swimming speed and duration (Fish and Hui, 1991). The maximum speed of 6.09 ms⁻¹ for a swimming period of 50 s (Lang and Norris, 1966) is representative of the speed and swimming duration of *Tursiops* in the present study.

The posterior one-third of the body was bent to effect dorsoventral movement of the flukes. Maximum amplitude was confined to the tips of the flukes. Flukes showed both spanwise and chordwise flexibility at the tips. During the upstrokes, the fluke tips were bent down slightly from the plane of the fluke, whereas bending in the opposite direction was observed during the downstroke. Flukes followed a sinusoidal pathway (Fig. 2). There was no significant difference between average time of up- and downstrokes of the flukes (paired *t*-test). Throughout both up- and downstrokes, the flukes were continuously pitched, which changed α over the stroke cycle. The angle of attack increased rapidly at the initiation of up- and downstrokes and reached a maximum within the first third of the stroke. The end of the stroke was accompanied by a drop in α with the flukes oriented parallel to the direction of forward progression. Maximum α decreased linearly by 42% over the *U* range examined (Fig. 3) as described by the equation:

$$\alpha_{\max} = 23.17 - 1.85U. \quad (8)$$

The relationship between α_{\max} and *U* was significantly correlated ($r=0.46$; $P<0.001$).

The peak-to-peak amplitude, *A*, was not significantly correlated with *U* ($r=0.16$; $P>0.2$). Mean *A* was 0.53 ± 0.09 m (s.D.). This represents a length-specific amplitude of $0.20\pm 0.03L$.

The frequency of the propulsive cycle (*f*) increased linearly with speed (Fig. 4) with a significant correlation ($r=0.85$; $P<0.001$) according to the equation:

$$f = 0.47 + 0.37U. \quad (9)$$

The positive linear relationship between frequency and swimming speed for *Tursiops* is consistent with the results for other marine mammals that use hydrofoil propulsion (Davis *et al.* 1985; Feldkamp, 1987; Fish *et al.* 1988). Maximum *f* for *Tursiops* corresponded to tail-beat frequency at maximum voluntary muscular effort for dolphins pushing against a load cell (Goforth, 1990).

Thrust power, efficiency and drag coefficient

Individual data points from swimming kinematics were used to compute reduced frequencies (σ ; equation 3) and feathering parameters (θ ; equation 4). The mean value of

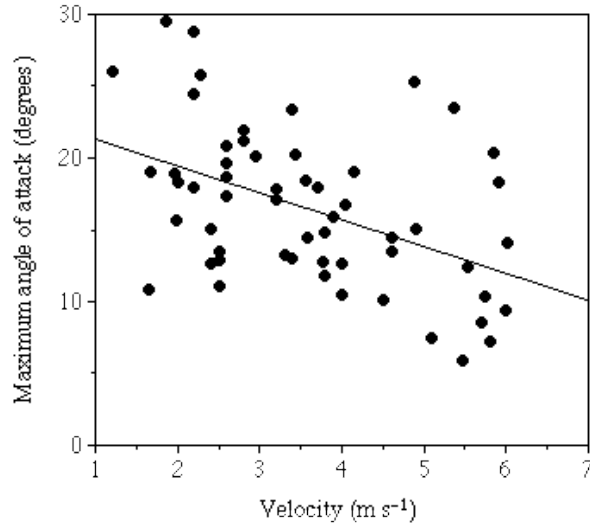


Fig. 3. Plot of the relationship between the maximum angle of attack, α_{\max} (degrees), and swimming velocity, U (m s^{-1}). Regression equation for line provided in text.

θ was calculated as 0.35 ± 0.11 . Values of σ were all over 0.5 (0.71 ± 0.17 ; range 0.51–1.15). Values of σ greater than 0.1 indicate that unsteady effects dominate the fluid forces associated with a propulsor such as an oscillating hydrofoil (Yates, 1983; Daniel and Webb, 1987). The data here are in accordance with those from other hydrofoil swimmers (Daniel and Webb, 1987).

The hydrodynamic model using unsteady lifting wing theory (Chopra and Kambe,

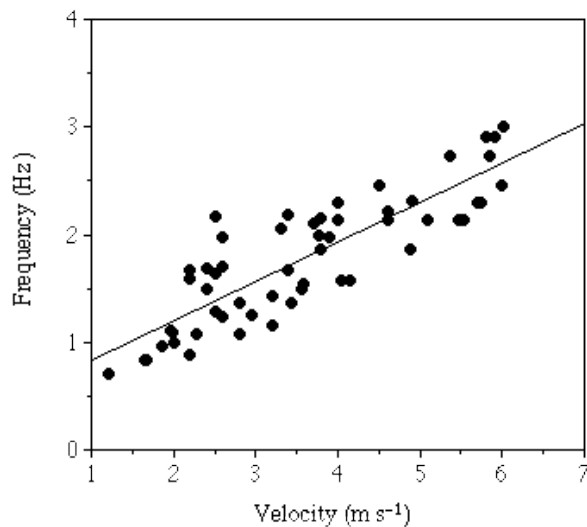


Fig. 4. Tail-beat frequency, f (Hz), as a function of the swimming velocity, U (m s^{-1}). Regression equation for line provided in text.

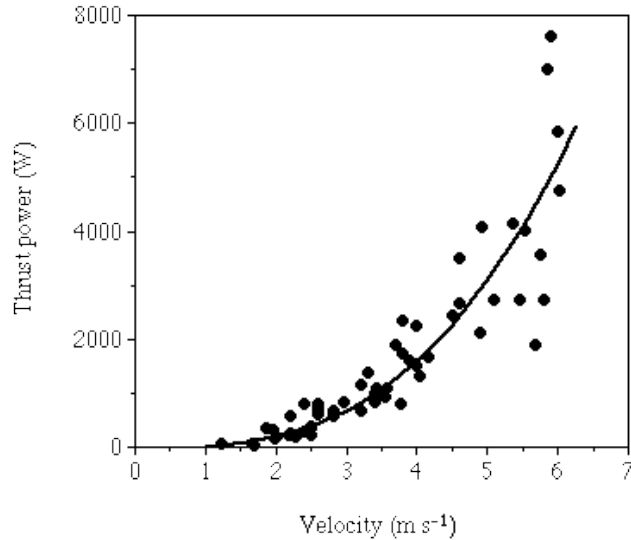


Fig. 5. The thrust power, P_T (W), as a function of the swimming velocity, U (m s^{-1}). Regression equation for line provided in text.

1977; Yates, 1983) related both C_T and η with σ for isopleths of θ . The calculated thrust power for *Tursiops* showed a curvilinear increase with increasing U (Fig. 5). Log-transformed data were used to compute a least-squares regression equation of:

$$P_T = 28.87U^{2.91}, \quad (10)$$

where P_T was measured in watts and U was measured in m s^{-1} . This equation was significantly correlated with U ($r=0.95$, $P<0.01$). The maximum P_T displayed by one of the dolphins swimming at 5.9 m s^{-1} ($2.2 L \text{ s}^{-1}$) was over 7600W.

No relationship was found for η with respect to U ($r=-0.13$; $P>0.2$). Mean η was 0.81 ± 0.04 , and η ranged from 0.73 to 0.91.

Computed values of dolphin C_D are compared with theoretical minimum drag coefficients in Fig. 6. For the dolphins, values of C_D not corrected for swimming depth varied from 0.006 to 0.046. Average C_D for dolphins was 6.95 times greater than the theoretical minimum drag coefficient (C_{Dm}) at equivalent Reynolds numbers. The C_{Dm} was calculated from an equation based on a rigid flat plate with turbulent boundary layer conditions (Webb, 1975). C_{Dm} assumes that the total drag is composed of a frictional component with no pressure drag component. However, the difference between theoretical and dolphin drag coefficients is decreased by 15.5% when the influence of shape and pressure drag are considered. In this case, theoretical drag coefficients (C_{Ds}) are based on streamlined bodies of revolution (Hoerner, 1965) with fineness ratios equal to that of the dolphins.

Depth-corrected drag coefficient, C_{Dd} , was on average 52% lower than C_D . Average C_{Dd} was 3.17 and 2.68 times greater than C_{Dm} and C_{Ds} , respectively. The lowest C_{Dd} computed was 0.0026 at an Re of 1.37×10^7 .

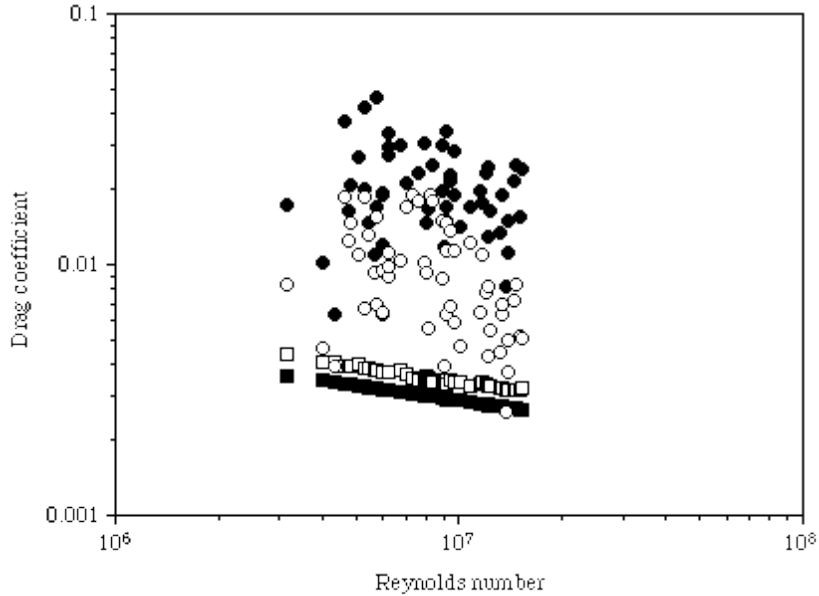


Fig. 6. Plot of drag coefficients, C_D , with respect to Reynolds number, Re . Individual values for C_D (●), C_{Dd} (○), C_{Dm} (■) and C_{Ds} (□) are shown. Theoretical drag coefficients assume turbulent boundary conditions exist. The relationship between C_D and Re is expressed by the equation $C_D=0.08Re^{-0.09}$ ($r=0.09$; $P>0.5$), and the relationship between C_{Dd} and Re is expressed by the equation $C_{Dd}=16.32Re^{-0.47}$ ($r=0.38$; $P<0.005$).

Discussion

The morphology and swimming kinematics of *Tursiops* are characteristic of the thunniform mode or carangiform with lunate tail (Lighthill, 1969, 1970; Lindsey, 1978; Fish *et al.* 1988). The thunniform mode is typical of some of the fastest marine vertebrates, including scombrid fishes, lamnid sharks and cetaceans (Lighthill, 1969). These species display morphological convergence for minimizing drag while maximizing thrust production. Body shape of these animals has a fineness ratio that approximates the optimal value of 4.5 for minimal drag and surface area with maximum volume (Hertel, 1966; Webb, 1975). The caudal peduncle exhibits extreme narrow necking in the plane of oscillation (Lighthill, 1969, 1970; Fish and Hui, 1991). Necking in the caudal region reduces virtual mass effects and unstable movements (Aleyev, 1977; Webb, 1975; Blake, 1983).

As with other thunniform swimmers, dolphins generate thrust exclusively with a high-aspect-ratio caudal hydrofoil (Fish and Hui, 1991). The tail flukes, which act as the hydrofoil, oscillate dorsoventrally while being pitched. Whereas changes in amplitude are accomplished by bending of the posterior one-third of the body, pitching is controlled at the base of the flukes. These heaving and pitching motions are responsible for changes of angle of attack and thrust generation throughout the stroke cycle (Lang and Daybell, 1963; Lighthill, 1969, 1970; Videler and Kamermans, 1985). Thrust is derived from a combination of the horizontal component of the lift force and leading-edge suction

(Ahmadi and Widnall, 1986). Thrust from lift increases directly with increases in angle of attack. However, low angles of attack increase hydromechanical efficiency while reducing the probability of stalling and decreased thrust production (Chopra, 1976). Excessive leading-edge suction could also induce stalling due to boundary layer separation, but the curved leading edge of the flukes (van Dam, 1987) should reduce leading-edge suction without a decrease in total thrust (Chopra and Kambe, 1977).

The three-dimensional hydromechanical model proposed by Chopra and Kambe (1977) provided reasonable estimates of P_T , although P_T may be an overestimate due the effects of the peduncle and small-aspect-ratio flukes. Values of P_T for *Tursiops* were, however, within the capacity of muscle power outputs for cruising and sprinting mammals (Webb, 1975). When compared on a mass-specific basis, *Tursiops* P_T was found to be equivalent to that of other marine mammals. The maximum mass-specific P_T for an individual *Tursiops* swimming at 5.85 ms^{-1} was 30.5 W kg^{-1} . This value was close to the maximum power output of 35.3 W kg^{-1} reported for *Stenella attenuata* (Lang and Pryor, 1966). Over a range of equivalent speeds, *Tursiops* had lower mass-specific P_T than *Lagenorhynchus obliquidens* (Lang, 1975), *Stenella attenuata* (Hui, 1987), phocid seals (Fish *et al.* 1988), *Zalophus californianus* and human runners (Feldkamp, 1987).

The propulsive efficiency was high for *Tursiops*, but within the range of η for other mammals that swim with an oscillating hydrofoil (Webb, 1975; Fish, 1992). Propulsive efficiencies range from 0.77 to 0.92 for otariid seals swimming with high-aspect-ratio foreflippers (Feldkamp, 1987) and dolphins and phocid seals swimming in the thunniform mode (Webb, 1975; Yates, 1983; Fish *et al.* 1988). The high efficiencies associated with these swimming modes are due to the maintenance of nearly continuous thrust production over the stroke cycle and a hydrofoil morphology which enhances high thrust with reduced drag (Fish, 1992).

Wu (1971) estimated that the propulsive efficiency of a dolphin could be as high as 0.99. This efficiency was assumed to be an overestimate because Wu used a two-dimensional analysis which underestimated trailing vorticity and wake energy loss (Ahmadi and Widnall, 1986; Karpouzian *et al.* 1990). Competing three-dimensional models of lunate tail swimming, including that of Chopra and Kambe (1977), predict efficiencies lower than 0.99 (Yates, 1983). However, efficiencies may be higher than predicted by all the models, because they assume that the hydrofoil is a rigid plate. Dolphin flukes exhibit both spanwise and chordwise flexibility (Joh, 1925; Felts, 1966; Purves, 1968; Curren, 1992). Katz and Weihs (1978) found that the chordwise flexibility of a foil increased propulsive efficiency by 20% with only a slight decrease in thrust compared with a rigid foil.

The tendency of the trained dolphins to swim near the water surface ($H/D < 3$) was largely responsible for the high power outputs and drag coefficients computed. Hertel (1966) showed that the drag on a body near the water surface could be up to five times higher than the drag on a body at a submerged depth greater than three times body diameter. Au and Weihs (1980) considered the maximum γ (drag augmentation factor) for a dolphin to be 4.5, because the dolphin is not an exact body of revolution. The increased drag is due to energy loss in the formation of waves (Lang and Daybell, 1963; Hertel, 1969; Fish, 1982). Wave drag is particularly important in marine mammals, which

are restricted to the surface because of respiratory requirements (Williams and Kooyman, 1985; Fish, 1992).

Swimming near the surface greatly increased drag coefficients for *Tursiops*. When corrected for swimming depth, C_{Dd} was 2.68–3.17 times greater than minimum theoretical drag coefficients. The higher drag coefficients for *Tursiops* were expected because the oscillating motions of the flukes and body while swimming will increase drag (Lighthill, 1971). The increased drag corresponds to thinning of the boundary layer, which increases skin friction over a greater proportion of the body than would occur for a rigid body of equal length. Lighthill (1971) estimated that skin friction could increase by up to a factor of five for undulating animals. The pressure component of drag would increase because of deviation from the streamlined body form due to the high-amplitude motions of the posterior body (Williams and Kooyman, 1985; Fish *et al.* 1988). An additional drag component, induced drag, would occur as a consequence of lift generation by the oscillating flukes. The induced drag component is the energy lost from tip vortices that are generated by pressure differences between the two sides of the flukes (Webb, 1975). The induced drag is highly dependent on AR , with high drag associated with low- AR untapered hydrofoils. Wall effects and swimming along a curved path would also contribute to high drag coefficients for *Tursiops*. Dolphins swimming in circles in small-radius (3.3m) pools had higher calculated power outputs than for linear swimming (Hui, 1987). However, by using banking to swim along a curved path, the additional drag for a neutrally buoyant dolphin would be low because there is no added induced drag from the flippers (Weihs, 1981). In the present study, the size and configurations of the pools and the distance from the wall that dolphins maintained should not have augmented drag significantly.

C_{Dd} averaged 3.2 and 20.2 times higher than the minimum drag coefficient with turbulent and laminar boundary conditions, respectively. These differences are large enough to be insensitive to any inaccuracies in calculation of thrust and drag, although estimates of thrust and drag should be considered conservative. Chopra and Kambe (1977) lowered their computed drag coefficient by 20% to correct for the effects of the peduncle and low AR . Such a correction for C_D in the present study still yields an average C_{Dd} 2.54 times C_{Dm} with a turbulent boundary layer. Such results are in agreement with drag coefficients measured or calculated previously for dolphins using thrust-based models (Lang and Daybell, 1963; Purves *et al.* 1975; Webb, 1975; Aleyev, 1977; Yates, 1983; Videler and Kamermans, 1985) (Fig. 7), but these results indicate that calculations using simple rigid-body analogies will underestimate the drag and power requirements of a swimming dolphin.

The idea that dolphins can minimize the drag by special mechanisms that maintain a laminar boundary layer (Gray, 1936; Kramer, 1960) has been of considerable interest (Fish and Hui, 1991). However, the results of numerous studies on dolphin hydrodynamics showed no special mechanisms for drag reduction. Drag is minimized primarily by a streamlined body design, with no known contribution from compliant viscous dampening, dermal ridges, secretions, boundary layer heating, or skin folds (Fish and Hui, 1991). Dolphins appear to maintain a turbulent boundary layer incurring higher

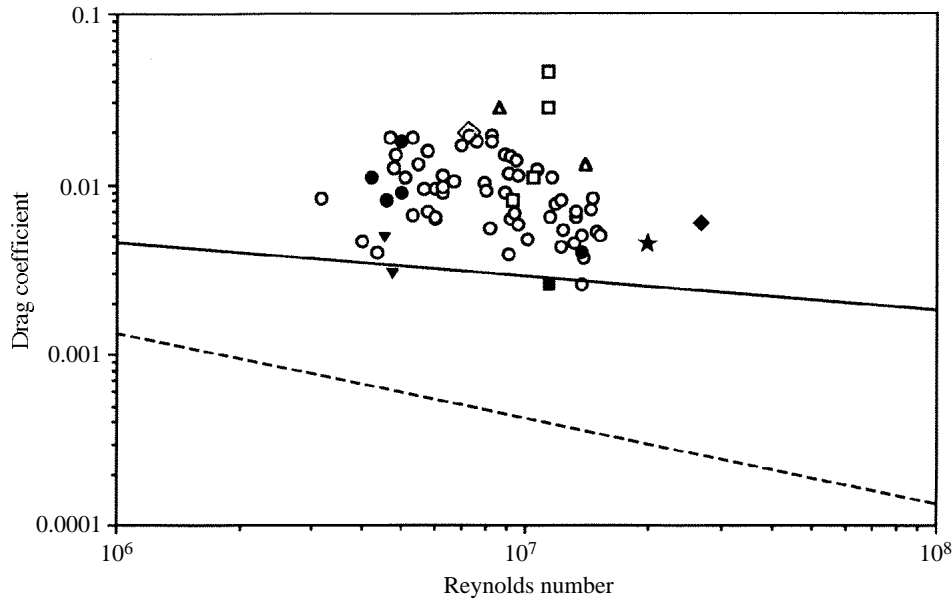


Fig. 7. Comparison of cetacean drag coefficients estimated from hydromechanical models based on kinematics and rigid bodies. Drag coefficients are plotted against Reynolds number, Re . Open circles represent depth-corrected drag coefficients, C_{Dd} , for *Tursiops truncatus* from this study. Other symbols represent *Delphinus delphis* (◆ and ◇), *Lagenorhynchus obliquidens* (■ and □), *Phocoena phocoena* (▲), *Phocoenoides dalli* (△), *Sotalia fluviatilis* (▼), *Stenella attenuata* (★) and *Tursiops truncatus* (●). Open symbols represent values of drag coefficient estimated using hydromechanical models based on swimming kinematics; filled symbols represent values obtained from gliding or towing experiments. Data are from Lang and Daybell (1963), Lang and Pryor (1966), Purves *et al.* (1975), Webb (1975), Aleyev (1977), Chopra and Kambe (1977), Yates (1983) and Videler and Kamermans (1985). The solid line represents the minimum drag coefficient assuming turbulent boundary conditions; the broken line is for minimum drag coefficient assuming laminar conditions.

drag and energy costs in swimming (Lang and Daybell, 1963; Videler and Kamermans, 1985; this study).

The highly derived swimming mode of dolphins allows for sufficient thrust generation to compensate for the drag incurred by the animal. Energy costs associated with turbulent boundary conditions and muscular performance within physiological norms restrict swimming performance. High-speed swimming is limited to the power that the animal can generate (Bose and Lien, 1989) and, while energetically possible in dolphins, high speeds are limited to bursts of short duration (Lang, 1975; Lockyer and Morris, 1987). Lunate-tail propulsion is associated with rapid and relatively high-powered swimming, but increased performance in dolphins is often the result of behavioral strategies that reduce energetic effort (Fish and Hui, 1991; Williams *et al.* 1992). The independently derived conclusion that dolphins have the capacity for high rates of work, but show no unusual hydrodynamic or physiological performance, is in agreement with the conclusions of Lang and Daybell (1963) and Williams *et al.* (1993).

I am extremely grateful to Sea World of Florida and the National Aquarium for providing the animals and assistance for this study. I am indebted particularly to S. Aibel, C. Andrews, K. Atlee, S. Berg, J. Fasick, D. Feuerbach, D. Gomersall, S. Hunter, J. Jarkoweic, R. Jenkins, J. McCoy, D. Odell, M. Osborn, D. Putnam, C. Thomas, C. Thompkins, J. Ventre, A. Weaver, R. West, R. White and D. Whitter. I also would like to thank C. A. Hui, T. M. Williams and two anonymous referees for their thorough and insightful comments on the text, R. G. Van Gelder for use of equipment and J. W. Weaver for technical assistance. This research was supported by NSF grant DCB-9117274 and by College of Arts and Sciences Support and Development Award, West Chester University.

References

- AHMADI, A. R. AND WIDNALL, S. E. (1986). Energetics and optimum motion of oscillating lifting surfaces of finite span. *J. Fluid Mech.* **162**, 261–282.
- ALEYEV, Y. G. (1977). *Nekton*. The Hague: Junk.
- ANDERSEN, S. H. (1981). Body surface area of juvenile harbour porpoise, *Phocoena phocoena*. *Aquat. Mamm.* **8**, 94–95.
- AU, D. AND PERRYMAN, W. (1982). Movement and speed of dolphin schools responding to an approaching ship. *Fish. Bull. Fish Wildl. Serv. U.S.* **80**, 371–379.
- AU, D. AND WEIHS, D. (1980). At high speeds dolphins save energy by leaping. *Nature* **284**, 548–550.
- BLAKE, R. W. (1983). *Fish Locomotion*. London: Cambridge University Press.
- BOSE, N. AND LIEN, J. (1989). Propulsion of a fin whale (*Balaenoptera physalus*): why the fin whale is a fast swimmer. *Proc. R. Soc. Lond. B* **237**, 175–200.
- BOSE, N., LIEN, J. AND AHIA, J. (1990). Measurements of the bodies and flukes of several cetacean species. *Proc. R. Soc. Lond. B* **242**, 163–173.
- CHOPRA, M. G. (1976). Large amplitude lunate-tail theory of fish locomotion. *J. Fluid Mech.* **74**, 161–182.
- CHOPRA, M. G. AND KAMBE, T. (1977). Hydrodynamics of lunate-tail swimming propulsion. Part 2. *J. Fluid Mech.* **79**, 49–69.
- CURREN, K. C. (1992). Designs for swimming: Morphometrics and swimming dynamics of several cetacean species. MS thesis, Memorial University of Newfoundland, 206pp.
- DANIEL, T. L. AND WEBB, P. W. (1987). Physical determinants of locomotion. In *Comparative Physiology: Life in Water and on Land* (ed. P. Dejours, L. Bolis, C. R. Taylor and E. R. Weibel), pp. 343–369. New York: Liviana Press.
- DAVIS, R. W., WILLIAMS, T. M. AND KOOYMAN, G. L. (1985). Swimming metabolism of yearling and adult harbor seals *Phocavitulina*. *Physiol. Zool.* **58**, 590–596.
- FELDKAMP, S. D. (1987). Swimming in the California sea lion: morphometrics, drag and energetics. *J. exp. Biol.* **131**, 117–135.
- FELTS, W. J. L. (1966). Some functional and structural characteristics of cetaceans flippers and flukes. In *Whales, Dolphins and Porpoises* (ed. K. S. Norris), pp. 255–276. Berkeley: University of California Press.
- FIERSTINE, H. L. AND WALTERS, V. (1968). Studies of locomotion and anatomy of scombrid fishes. *Mem. S. Calif. Acad. Sci.* **6**, 1–31.
- FISH, F. E. (1982). Aerobic energetics of surface swimming in the muskrat *Ondatra zibethicus*. *Physiol. Zool.* **55**, 180–189.
- FISH, F. E. (1992). Aquatic locomotion. In *Mammalian Energetics: Interdisciplinary Views of Metabolism and Reproduction* (ed. T. E. Tomasi and T. H. Horton), pp. 34–63. Ithaca, New York: Cornell University Press.
- FISH, F. E. AND HUI, C. A. (1991). Dolphin swimming – a review. *Mamm. Rev.* **21**, 181–195.
- FISH, F. E., INNES, S. AND RONALD, K. (1988). Kinematics and estimated thrust production of swimming harp and ringed seals. *J. exp. Biol.* **137**, 157–173.
- GOFORTH, H. W. (1990). Ergometry (exercise testing) of the bottlenose dolphin. In *The Bottlenose Dolphin* (ed. S. Leatherwood), pp. 559–574. New York: Academic Press.

- GRAY, J. (1936). Studies in animal locomotion. VI. The propulsive powers of the dolphin. *J. exp. Biol.* **13**, 192–199.
- HAMPTON, I. F. G., WHITTOW, G. C., SZEKERCZES, J. AND RUTHERFORD, S. (1971). Heat transfer and body temperature in the Atlantic bottlenose dolphin, *Tursiops truncatus*. *Int. J. Biometeor.* **15**, 247–253.
- HERTEL, H. (1966). *Structure, Form and Movement*. New York: Rheinhold.
- HERTEL, H. (1969). Hydrodynamics of swimming and wave-riding dolphins. In *The Biology of Marine Mammals* (ed. H. T. Andersen), pp. 31–63. New York: Academic Press.
- HOERNER, S. F. (1965). *Fluid-dynamic Drag*. Midland Park, NJ: Published by the author.
- HUI, C. A. (1987). Power and speed of swimming dolphins. *J. Mammal.* **68**, 126–132.
- JOH, C. G. (1925). The motion of whales during swimming. *Nature* **116**, 327–329.
- KANWISHER, J. AND SUNDNES, G. (1966). Thermal regulation in cetaceans. In *Whales, Dolphins and Porpoises* (ed. K. Norris), pp. 398–409. Berkeley: University of California Press.
- KARPOUZIAN, G., SPEDDING, G. AND CHENG, H. K. (1990). Lunate-tail swimming propulsion. Part 2. Performance analysis. *J. Fluid Mech.* **210**, 329–351.
- KATZ, J. AND WEIHS, D. (1978). Hydrodynamic propulsion by large amplitude oscillation of an airfoil with chordwise flexibility. *J. Fluid Mech.* **88**, 485–497.
- KRAMER, M. (1960). The dolphin's secret. *New Sci.* **7**, 1118–1120.
- LANG, T. G. (1975). Speed, power and drag measurements of dolphins and porpoises. In *Swimming and Flying in Nature* (ed. T. Y. Wu, C. J. Brokaw and C. Brennen), pp. 553–571. New York: Plenum Press.
- LANG, T. G. AND DAYBELL, D. A. (1963). Porpoise performance tests in a seawater tank. *Nav. Ord. Test Sta. Tech. Rep.* **3063**, 1–50.
- LANG, T. G. AND NORRIS, K. S. (1966). Swimming speed of a Pacific bottlenose porpoise. *Science* **151**, 588–590.
- LANG, T. G. AND PRYOR, K. (1966). Hydrodynamic performance of porpoises (*Stenella attenuata*). *Science* **152**, 531–533.
- LIGHTHILL, M. J. (1969). Hydrodynamics of aquatic animal propulsion. *A. Rev. Fluid Mech.* **1**, 413–446.
- LIGHTHILL, M. J. (1970). Aquatic animal propulsion of high hydromechanical efficiency. *J. Fluid Mech.* **44**, 265–301.
- LIGHTHILL, M. J. (1971). Large-amplitude elongated-body theory of fish locomotion. *Proc. R. Soc. Lond. B* **179**, 125–138.
- LINDSEY, C. C. (1978). Form, function and locomotory habits in fish. In *Fish Physiology: Locomotion*, vol. VII (ed. W. S. Hoar and D. J. Randall), pp. 1–100. New York: Academic Press.
- LOCKYER, C. AND MORRIS, R. (1987). Observation on diving behaviour and swimming speeds in a wild juvenile *Tursiops truncatus*. *Aquat. Mamm.* **13**, 31–35.
- NORRIS, K. S. AND PRESCOTT, J. H. (1961). Observations of Pacific cetaceans of California and Mexican waters. *Univ. Calif. Publ. Zool.* **63**, 291–402.
- PARRY, D. A. (1949). The swimming of whales and a discussion of Gray's paradox. *J. exp. Biol.* **26**, 24–34.
- PURVES, P. E. (1968). The structure of the flukes in relation to laminar flow in cetaceans. *Z. Saugetierkunde*, **33**, 1–8.
- PURVES, P. E., DUDOKVAN HEEL, W. H. AND JONK, A. (1975). Locomotion in dolphins. I. Hydrodynamic experiments on a model of the bottle-nosed dolphin, *Tursiops truncatus* (Mont.). *Aquat. Mamm.* **3**, 5–31.
- RIDGWAY, S. H. (1972). *Mammals of the Sea, Biology and Medicine*. Springfield, Illinois: C. C. Thomas.
- SLIJPER, E. J. (1958). Organ weights and symmetry problems in porpoises and seals. *Arch. neerl. Zool.* **13**, 97–113.
- SLIJPER, E. J. (1961). Locomotion and locomotory organs in whales and dolphins (Cetacea). *Symp. zool. Soc. Lond.* **5**, 77–94.
- VAN DAM, C. P. (1987). Efficiency characteristics of crescent-shaped wings and caudal fins. *Nature* **325**, 435–437.
- VIDELER, J. AND KAMERMANS, P. (1985). Differences between upstroke and downstroke in swimming dolphins. *J. exp. Biol.* **119**, 265–274.
- WEBB, P. W. (1975). Hydrodynamics and energetics of fish propulsion. *Bull. Fish. Res. Bd Can.* **190**, 1–159.
- WEIHS, D. (1981). Effects of swimming path curvature on the energetics of fish motion. *Fish. Bull. Fish Wildl. Serv. U.S.* **79**, 171–176.

- WILLIAMS, T. M., FRIEDL, W. A., FONG, M. L., YAMADASEDIVY, P. AND HAUN, J. E. (1992). Travel at low energetic cost by swimming and wave-riding bottlenose dolphins. *Nature* **355**, 821–823.
- WILLIAMS, T. M., FRIEDL, W. A. AND HAUN, J. E. (1993). The physiology of bottlenose dolphins (*Tursiops truncatus*): heart rate, metabolic rate and plasma lactate concentration during exercise. *J. exp. Biol.* **179**, 31–46.
- WILLIAMS, T. M. AND KOOYMAN, G. L. (1985). Swimming performance and hydrodynamic characteristics of harbor seals *Phocavitulina*. *Physiol. Zool.* **58**, 576–589.
- WU, T. Y. T. (1971). Hydromechanics of swimming propulsion. Part 2. Some optimum shape problems. *J. Fluid Mech.* **46**, 521–544.
- WURSIG, B. AND WURSIG, M. (1979). Behavior and ecology of the bottlenose dolphin, *Tursiops truncatus*, in the South Atlantic. *Fish. Bull. Fish Wildl. Serv. U.S.* **77**, 399–412.
- YASUI, W. Y. (1980). Morphometrics, hydrodynamics and energetics of locomotion for a small cetacean, *Phocoena phocoena* (L.). MSc thesis, University of Guelph, Ontario.
- YATES, G. T. (1983). Hydrodynamics of body and caudal fin propulsion. In *Fish Biomechanics* (ed. P. W. Webb and D. Weihs), pp. 177–213. New York: Praeger.